FERMILAB-CONF-14-394-T

Available online at www.sciencedirect.com

ScienceDirect

Nuclear Physics B Proceedings Supplement 00 (2014) 1–6

Nuclear Physics B Proceedings Supplement

Constraining the top-Z coupling through $t\bar{t}Z$ production at the LHC

Raoul Röntsch[1]

Fermilab, PO Box 500, Batavia, IL 60510, USA

Markus Schulze

PH Department, TH Unit, CERN, 1211 Geneva 23, Switzerland

Abstract

We study top pair production in association with a Z-boson at the LHC, focusing on the sensitivity to the top-Z couplings. As yet, these couplings have not been studied in a hadronic collider environment. We calculate $t\bar{t}Z$ production to next-to-leading order in perturbative QCD, and include spin correlations in the top and Z-decays to the same order. We use the cross section measurements made by CMS using 4.9 fb^{-1} of data from the $\sqrt{s} = 7$ TeV LHC run to place constraints on the top-Z couplings through a log-likelihood ratio analysis. Looking ahead to the higher energy run, we use the azimuthal angle between the leptons arising from the Z-decay, which is particularly sensitive to the top-Z coupling, to investigate the constraints that could be obtained using 30, 300, and 3000 fb^{-1} of data. We find that using NLO predictions significantly improves the top-Z coupling constraints, due to the decreased scale uncertainty.

Keywords: Top physics, NLO Computations, QCD Phenomenology

1. Introduction

The top quark is the heaviest known elementary particle, and, while several of its properties are well understood, its interactions with the electroweak sector have yet to be studied in hadronic collisions. The observation that the top Yukawa coupling $y_t \sim 1$ suggests that the top may have a special role to play in electroweak symmetry breaking (EWSB); more generally, one would expect that the interactions between the top and the electroweak sector are sensitive to the EWSB mechanism. Thus a full understanding of EWSB requires an understanding of the top-electroweak couplings. In this work, we focus on the vector and axial top-Z couplings in particular. Indirect constraints on these couplings [1, 2, 3] can be obtained from LEP data [4, 5], but as yet there is no constraint from a direct measurement. Such a constraint can be obtained from $t\bar{t}Z$ production at the LHC, which has a cross section of approximately 1 pb at $\sqrt{s} = 13$ TeV. Indeed, a few $t\bar{t}Z$ events have been observed by both CMS [6] and ATLAS [7] during the lower energy runs. With higher energies and integrated luminosities, the sample size is anticipated to be large enough to allow coupling measurements to be made.

Email addresses: rontsch@fnal.gov (Raoul Röntsch), markus.schulze@cern.ch (Markus Schulze)

[1] Speaker

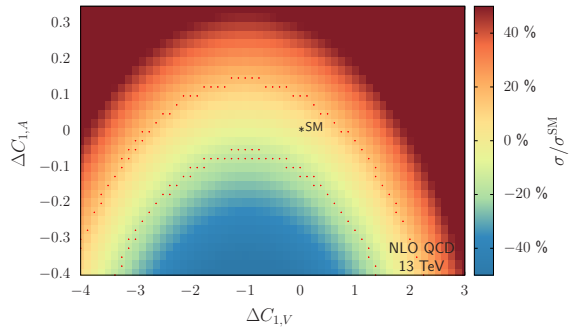

Figure 1: Relative deviations of the NLO QCD cross section as a function of relative shifts in vector and axial couplings $\Delta C_{1,V}$ and $\Delta C_{1,A}$.

How well the top-Z coupling can be constrained is dependent not only on experimental factors, but also on the theoretical understanding of the $pp \to t\bar{t}Z$ process. This point was highlighted in Refs. [8, 9], which investigated the capability of the LHC to constrain the top-Z coupling using leading-order (LO) distributions. At this order, the scale uncertainty is 30%, and this was identified as the biggest theoretical obstacle to obtaining better coupling constraints from this process. To reduce this uncertainty, it is necessary to use next-to-leading order (NLO) theoretical predictions in the analysis. This is the aim of a recent work by the authors [10], upon which this talk is based.

2. Details of calculation

We are interested in the hadroproduction of $t\bar{t}Z$, focusing on the trileptonic decay channel. We therefore perform a partonic-level calculation of the process $pp \to t\bar{t}+Z \to t(\to \ell\nu b)\,\bar{t}(\to jj\bar{b})\,Z(\to \ell\ell)$ to NLO in perturbative QCD. The opening angle between the leptons arising from the Z-decay $\Delta\phi_{\ell\ell}$ displays shape sensitivity to the top-Z couplings [8], and we will make extensive use of this in our analysis. For this reason, we include all spin correlations in the decays to NLO, and work in the narrow-width approximation for both the top quark and the Z-boson. In addition to providing accurate predictions for spin variables, this allows us to include realistic experimental cuts on the final state objects.

Deviations of the top-Z couplings from their Standard Model (SM) values can be conveniently expressed in an effective field theory (EFT), where the top-Z Lagrangian is written in terms of higher dimensional operators suppressed by a scale Λ which characterizes the new physics. Limiting ourselves to dimension-six operators and assuming an SU(2) symmetry, these can be translated to four anomalous couplings $C_{1/2,V/A}$, and the Lagrangian becomes [11]

$$\mathcal{L}_{t\bar{t}Z} = e\bar{u}(p_t)\left[\gamma^\mu\left(C_{1,V} + \gamma_5 C_{1,A}\right) + \frac{\mathrm{i}\sigma_{\mu\nu}q_\nu}{M_Z}\left(C_{2,V} + \mathrm{i}\gamma_5 C_{2,A}\right)\right]v(p_{\bar{t}})Z_\mu, \tag{1}$$

with $q_\nu = (p_t - p_{\bar{t}})_\nu$. The couplings $C_{1/2,V/A}$ are independent of the external momentum. In the SM, we have

$$C_{1,V} = C_V^{\mathrm{SM}} = \frac{T^3 - 2Q_t \sin^2\theta_w}{2\sin\theta_w\cos\theta_w}, \qquad C_{1,A} = C_A^{\mathrm{SM}} = \frac{-T^3}{2\sin\theta_w\cos\theta_w}. \tag{2}$$

The remaining two couplings, $C_{2,V/A}$, correspond to the top magnetic and electric dipole moments. Their values are zero at tree-level in the SM and receive only small higher-order corrections [12, 13]. For the purposes of this work, $C_{2,V/A}$ are kept at their SM value of zero, and we focus solely on variations of $C_{1,V/A}$ from their SM values.

3. Results

3.1. NLO QCD results

We first present results at LO and NLO in QCD using SM values of the top-Z couplings, before investigating the impact of varying these couplings. We shall present results at a factorization and renormalization scale $\mu_0 = m_t + m_Z/2$, and use the MSTW2008 distributions throughout [14].

At the $\sqrt{s} = 7$ TeV LHC, we find inclusive cross sections at LO and NLO of $\sigma^{\text{LO}}_{t\bar{t}Z} = 103.5$ fb and $\sigma^{\text{NLO}}_{t\bar{t}Z} = 137.0$ fb, in agreement with the results of Ref. [15]. The inclusive cross section at $\sqrt{s} = 13$ TeV increases significantly to approximately 1 pb. A realistic idea of the number of events can be obtained by including decays in the trileptonic channel, $t\bar{t}Z \to (jjb\bar{b}\ell\nu\ell^+\ell^-)$, and imposing fairly inclusive cuts on the final state products:

$$\begin{aligned} p^{\ell}_{\text{T}} &\geq 15 \text{ GeV}, \quad |y^{\ell}| \leq 2.5, \\ p^{j}_{\text{T}} &\geq 20 \text{ GeV}, \quad |y^{j}| \leq 2.5, \\ p^{\text{miss}}_{\text{T}} &\geq 20 \text{ GeV}, \quad R_{\ell j} \geq 0.4, \end{aligned} \tag{3}$$

where jets are defined by the anti-k_{T} algorithm [16] with $R = 0.4$. With these cuts the cross-sections are

$$\sigma^{\text{LO}}_{t\bar{t}Z} = 3.79(0)^{+34\%}_{-25\%} \text{ fb}, \qquad \sigma^{\text{NLO}}_{t\bar{t}Z} = 5.16(1)^{+13\%}_{-12\%} \text{ fb}. \tag{4}$$

The scale uncertainties are obtained by varying the central scale μ_0 by a factor of 2 in either direction. The scale uncertainty is approximately 28% at LO and reduces to 13% at NLO. This reduction will prove invaluable when constraining the top-Z couplings. We also note that $k = \sigma^{\text{NLO}}_{t\bar{t}Z}/\sigma^{\text{LO}}_{t\bar{t}Z} \simeq 1.4$. This relatively large value is due to the qg and $\bar{q}g$ channels opening at NLO.

3.2. Top-Z coupling constraints

We now proceed to the main purpose of this work, namely to investigate direct constraints on the top-Z coupling that can be obtained from the LHC. We vary the couplings $C_{1,V}$ and $C_{1,A}$ of Eq. (1), but keep all other couplings at their SM value (in particular, the couplings of the Z-boson to the light quarks is unchanged). This requires NLO calculations for a large number of points in $(C_{1,V}, C_{1,A})$ parameter space. In order to save computational time, we observe that any amplitude that we need to calculate has the form

$$\mathcal{A}_{t\bar{t}Z} = A_0 + A_V C_{1,V} + A_A C_{1,A}, \tag{5}$$

where all other couplings, kinematics, etc. are in the coefficients A_0, A_V, and A_A. A differential cross section can then be written as

$$d\sigma = s_0 + s_1 C_{1,V} + s_2 C^2_{1,V} + s_3 C_{1,A} + s_4 C^2_{1,A} + s_5 C_{1,V} C_{1,A}. \tag{6}$$

By computing the differential cross section at six points in $(C_{1,V}, C_{1,A})$ parameter space, we can solve for the coefficients s_i, and use these to generate cross sections as well as differential distributions for a large number of $(C_{1,V}, C_{1,A})$ points.

It is instructive to examine the dependence of the cross section on the top-Z couplings, for a large range of values of $C_{1,V}$ and $C_{1,A}$. This is shown at NLO in Fig. 1 for the 13 TeV LHC, with the relative coupling shifts defined as $\Delta C_{1,V} = C_{1,V}/C^{\text{SM}}_V - 1$ and $\Delta C_{1,A} = C_{1,A}/C^{\text{SM}}_A - 1$. Within the shown coupling ranges, the cross section varies by about ±50% relative to the SM value. The cross sections are roughly symmetric about the axis $\Delta C_{1,V} = -1$, which corresponds to $C_{1,V} = 0$. This can be understood by observing that the LO cross section is dominantly proportional to $C^2_{1,V} + C^2_{1,A}$. A similar symmetry is expected about $\Delta C_{1,A} = -1$, however the sign of the axial coupling is already constrained from LEP measurements of the $Zb_{\text{L}}\bar{b}_{\text{L}}$ interaction when $\text{SU}(2)_{\text{L}}$ symmetry is invoked, and consequently we do not show the results for a negative value of $C_{1,A}$ here. The dotted line in Fig. 1 indicates a deviation from the SM cross section by ±15%, which is the approximate scale uncertainty at NLO. Thus, any coupling point within these lines cannot be distinguished from the SM by its rate alone. This includes couplings far from the SM values, e.g. $(\Delta C_{1,V}, \Delta C_{1,A}) = (1.7, -0.3)$. We will see that adding shape information improves the situation and leads to a more powerful discrimination.

To analyze the ability of the LHC experiments to distinguish between different points in $(\Delta C_{1,V}, \Delta C_{1,A})$ parameter space, we make use of a binned log-likelihood ratio analysis. This allows us to identify two points in the parameter space as competing hypotheses, and to compare distributions obtained under each. When comparing two distributions, we include the effects of the scale uncertainty by varying both overall cross sections within the scale uncertainty bands so as to minimize their difference. For further details, we refer the reader to Ref. [10].

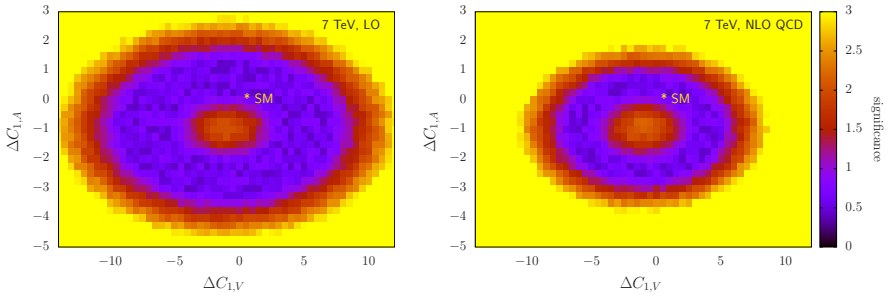

Figure 2: Significance as a function of relative deviations for vector and axial couplings $\Delta C_{1,V}$ and $\Delta C_{1,A}$. The limits are obtained from the first measurement of the $t\bar{t}Z$ cross section by CMS [6]. The left (right) plot shows the limits obtained from LO (NLO) QCD input.

The first $t\bar{t}Z$ events were seen at the $\sqrt{s} = 7$ TeV run. CMS observed 9 events with 4.9 fb^{-1} of data [6]; ATLAS, using more restrictive acceptance cuts, observed a single event in 4.7 fb^{-1} of data [7]. This enabled CMS to extrapolate a total inclusive $t\bar{t}Z$ cross-section

$$\sigma_{t\bar{t}Z} = 0.28^{+0.14}_{-0.11}\ (\text{stat.})\ ^{+0.06}_{-0.03}\ (\text{sys.})\ \text{pb}, \tag{7}$$

which is in good agreement with our previously quoted NLO cross section of 0.137 pb. In spite of the low number of events and correspondingly high statistical error, it is instructive to use this measured cross section to place bounds on the $t\bar{t}Z$ couplings. The null hypothesis in our log-likelihood ratio analysis is the experimental cross section, and we confront this with an alternate hypothesis, which is the cross section obtained using a given point in $(\Delta C_{1,V}, \Delta C_{1,A})$ parameter space. The theoretical uncertainties, which are a combination of the scale and pdf uncertainties, are 40% at LO and 15% at NLO. The effects of the 20% experimental systematic uncertainty are taken into account with a Gaussian distributed probability.

The results are shown in Fig. 2 for LO and NLO results. The color code indicates the significance with which a given point in $(\Delta C_{1,V}, \Delta C_{1,A})$ parameter space can be excluded with respect to the experimental data. We note that the SM cross section, which corresponds to the point $(\Delta C_{1,V}, \Delta C_{1,A}) = (0, 0)$, is fully consistent with the experimental value. The lower theoretical uncertainty at NLO leads to tighter constraints, which are immediately apparent. Even so, the limits are extremely loose, and furthermore should be interpreted with care since very few events have been observed by the experiments so far.

In order to improve upon these limits, we turn now to the $\sqrt{s} = 13$ TeV run of the LHC, and consider the potential limits that could be set given 30, 300, or 3000 fb^{-1} of data. For this analysis, we make use of the $\Delta\phi_{\ell\ell}$ distribution, which was identified in Ref. [8] as being particularly sensitive to the top-Z couplings. Since there are obviously no data at this energy yet, we adopt our theoretical prediction using the SM couplings as our null hypothesis, and a point in $(\Delta C_{1,V}, \Delta C_{1,A})$ space as our alternate hypothesis. We thus compute a statistical separation between the SM point $(\Delta C_{1,V}, \Delta C_{1,A}) = (0, 0)$ and a point $(\Delta C_{1,V}, \Delta C_{1,A}) \neq (0, 0)$. Assuming that the data, once available, are in agreement with the SM predictions, our results indicate the approximate experimental bounds that may be achieved.

In Fig. 3, we show the constraints for 30, 300, and 3000 fb^{-1} of data, using LO and NLO results. The scale uncertainty is 30% at LO and 15% at NLO. We see an obvious and expected improvement as the luminosity is increased, as well as a significant improvement when using the NLO results, driven again by the lower scale uncertainty. Focusing on the bounds from 300 fb^{-1}, the LO constraints are $-4.0 < \Delta C_{1,V} < 2.8$ and $-0.36 < \Delta C_{1,A} < 0.54$, while at NLO these limits become $-3.6 < \Delta C_{1,V} < 1.6$ and $-0.24 < \Delta C_{1,A} < 0.30$. In terms of absolute values, these intervals correspond to $C_{\text{V}} = 0.24^{+0.39}_{-0.85}$ and $C_{\text{A}} = -0.60^{+0.14}_{-0.18}$ at NLO QCD. We also note that the shape information allows us exclude regions in parameter space which could not be excluded based on the cross sections alone.

Finally, we can express the above constraints on $\Delta C_{1,V}$ and $\Delta C_{1,A}$ as constraints on dimension-six operators in an EFT. Ref. [11] gives

$$C_{1,V} = C_{1,V}^{\text{SM}} + \left(\tfrac{v^2}{\Lambda^2}\right) \text{Re}\left[C_{\phi q}^{(3,33)} - C_{\phi q}^{(1,33)} - C_{\phi u}^{33}\right], \tag{8}$$

$$C_{1,A} = C_{1,A}^{\text{SM}} + \left(\tfrac{v^2}{\Lambda^2}\right) \text{Re}\left[C_{\phi q}^{(3,33)} - C_{\phi q}^{(1,33)} + C_{\phi u}^{33}\right], \tag{9}$$

and further imposing an SU(2) gauge symmetry gives the relation $C_{\phi q}^{(3,33)} \approx -C_{\phi q}^{(1,33)}$. This allows us to translate the

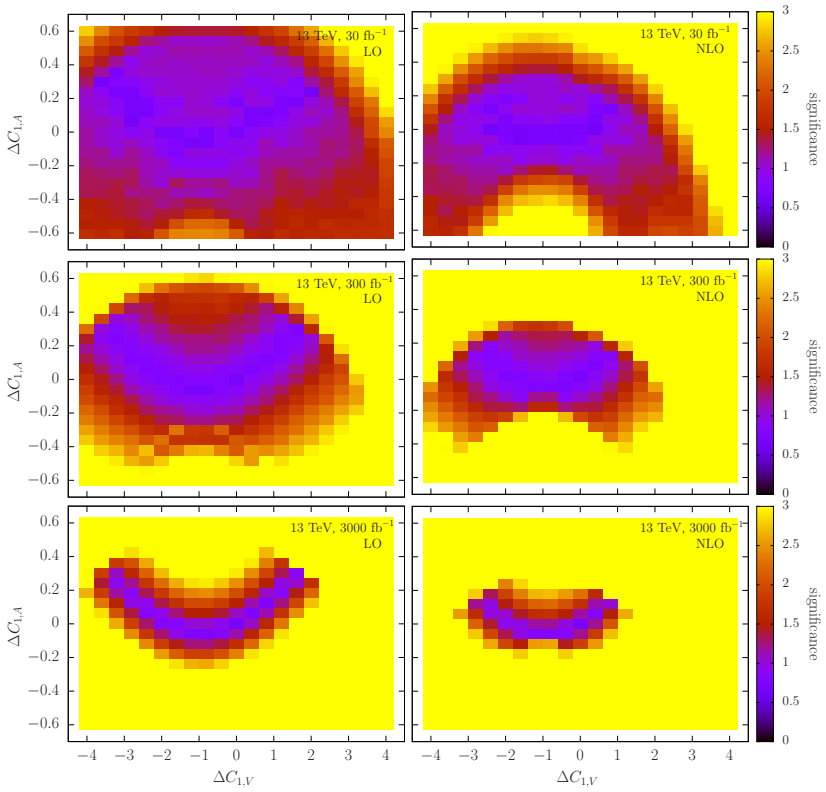

Figure 3: Significance as a function of relative deviations for vector and axial couplings $\Delta C_{1,V}$ and $\Delta C_{1,A}$, using the $\Delta\phi_{\ell\ell}$ distribution with 30, 300 and 3000 fb^{-1} of data at the $\sqrt{s} = 13$ TeV LHC. Results using the LO prediction and uncertainty are shown on the left, the corresponding NLO QCD results are shown on the right hand side.

above constraints on $\Delta C_{1,V}$ and $\Delta C_{1,A}$ into constraints on $C_{\phi q}^{(3,33)}$ and $C_{\phi u}^{33}$, shown in Fig. 4. Also shown are the indirect constraints, obtained from LEP limits on ϵ_1 and ϵ_b which can be written in terms of operators following Ref. [17]. While it is clear that the direct constraints are not as strong as those obtained from LEP data, they also rely on fewer assumptions.

4. Conclusions

We have studied the top-Z coupling, using direct sensitivity in process $t\bar{t}Z$ at the LHC. Our calculation is performed to NLO in QCD, and takes into account all decays with full spin correlations at this order, within the narrow-width approximation. We use a log-likelihood ratio analysis of the first reported $t\bar{t}Z$ cross section measurement from CMS to place constraints on the top-Z coupling. Due to the low number of observed events, these constraints are statistically limited and hence very loose. Looking forward, we consider the $\sqrt{s} = 13$ TeV LHC run with 30, 300, and 3000 fb^{-1} of data, using the azimuthal angle between the leptons arising from the Z-decay to provide additional sensitivity through the shape information. We observe a significant improvement in the constraints when using the NLO prediction, due to the corresponding decrease in the scale uncertainty. We establish that the LHC should be able to constrain the top-Z couplings to $-3.6 < \Delta C_{1,V} < 1.6$ and $-0.24 < \Delta C_{1,A} < 0.30$ using 300 fb^{-1} of data and NLO QCD results. Writing these constraints in terms of higher dimension operators in an EFT allows us to interpret these results as model-independent constraints on new physics. We look forward to the observation of $t\bar{t}Z$ production at run II of the LHC, and the subsequent constraints on the top-Z couplings.

Acknowledgements

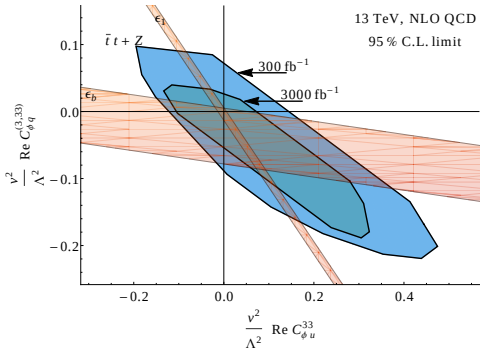

Figure 4: Projected constraints on the operators $C_{\phi q}^{(3,33)}$ and $C_{\phi u}^{33}$ obtained from the $\Delta\phi_{\ell\ell}$ distribution in $t\bar{t}Z$ production at the 13 TeV LHC. The parameter space outside the blue colored area can be excluded at the 95% C.L. The thin bands are indirect constraints from electroweak precision data.

RR would like to thank the organizers of ICHEP 2014 for a stimulating conference, and the convenors of the top/electroweak session in particular for the opportunity to present this work. We are thankful to the authors of Ref. [17] for discussions on the LEP constraints after this work was presented at ICHEP. Fermilab is operated by Fermi Research Alliance, LLC under Contract No. De-AC02-07CH11359 with the United States Department of Energy. This research used resources of the National Energy Research Scientific Computing Center, which is supported by the Office of Science of the U.S. Department of Energy under Contract No. DE-AC02-05CH11231.

References

[1] G. Altarelli, R. Barbieri, Vacuum polarization effects of new physics on electroweak processes, Phys.Lett. B253 (1991) 161–167. doi:10.1016/0370-2693(91)91378-9.
[2] G. Altarelli, R. Barbieri, S. Jadach, Toward a model independent analysis of electroweak data, Nucl.Phys. B369 (1992) 3–32. doi:10.1016/0550-3213(92)90376-M.
[3] G. Altarelli, R. Barbieri, F. Caravaglios, Nonstandard analysis of electroweak precision data, Nucl.Phys. B405 (1993) 3–23. doi:10.1016/0550-3213(93)90424-N.
[4] S. Schael, et al., Precision electroweak measurements on the Z resonance, Phys.Rept. 427 (2006) 257–454. arXiv:hep-ex/0509008, doi:10.1016/j.physrep.2005.12.006.
[5] J. Abdallah, et al., A Study of b anti-b Production in e+e- Collisions at s**(1/2) = 130-GeV - 207-GeV, Eur.Phys.J. C60 (2009) 1–15. arXiv:0901.4461, doi:10.1140/epjc/s10052-009-0917-2.
[6] S. Chatrchyan, et al., Measurement of associated production of vector bosons and top quark-antiquark pairs at sqrt(s) = 7 TeV, Phys.Rev.Lett. 110 (2013) 172002. arXiv:1303.3239, doi:10.1103/PhysRevLett.110.172002.
[7] Search for $t\bar{t}Z$ production in the three lepton final state with 4.7 fb^{-1} of $\sqrt{s} = 7$ TeV pp collision data collected by the ATLAS detector, Tech. Rep. ATLAS-CONF-2012-126, CERN, Geneva (Aug 2012).
[8] U. Baur, A. Juste, L. Orr, D. Rainwater, Probing electroweak top quark couplings at hadron colliders, Phys.Rev. D71 (2005) 054013. arXiv:hep-ph/0412021, doi:10.1103/PhysRevD.71.054013.
[9] U. Baur, A. Juste, D. Rainwater, L. Orr, Improved measurement of ttZ couplings at the CERN LHC, Phys.Rev. D73 (2006) 034016. arXiv:hep-ph/0512262, doi:10.1103/PhysRevD.73.034016.
[10] R. Rontsch, M. Schulze, Constraining couplings of top quarks to the Z boson in $t\bar{t}$ + Z production at the LHC, JHEP 1407 (2014) 091. arXiv:1404.1005, doi:10.1007/JHEP07(2014)091.
[11] J. Aguilar-Saavedra, A Minimal set of top anomalous couplings, Nucl.Phys. B812 (2009) 181–204. arXiv:0811.3842, doi:10.1016/j.nuclphysb.2008.12.012.
[12] J. Bernabeu, D. Comelli, L. Lavoura, J. P. Silva, Weak magnetic dipole moments in two Higgs doublet models, Phys.Rev. D53 (1996) 5222–5232. arXiv:hep-ph/9509416, doi:10.1103/PhysRevD.53.5222.
[13] W. Hollik, J. I. Illana, S. Rigolin, C. Schappacher, D. Stockinger, Top dipole form-factors and loop induced CP violation in supersymmetry, Nucl.Phys. B551 (1999) 3–40. arXiv:hep-ph/9812298, doi:10.1016/S0550-3213(99)00201-1.
[14] A. Martin, W. Stirling, R. Thorne, G. Watt, Parton distributions for the LHC, Eur.Phys.J. C63 (2009) 189–285. arXiv:0901.0002, doi:10.1140/epjc/s10052-009-1072-5.
[15] A. Kardos, Z. Trocsanyi, C. Papadopoulos, Top quark pair production in association with a Z-boson at NLO accuracy, Phys.Rev. D85 (2012) 054015. arXiv:1111.0610, doi:10.1103/PhysRevD.85.054015.
[16] M. Cacciari, G. P. Salam, G. Soyez, The Anti-k(t) jet clustering algorithm, JHEP 0804 (2008) 063. arXiv:0802.1189, doi:10.1088/1126-6708/2008/04/063.
[17] J. Brod, A. Greljo, E. Stamou, P. Uttayarat, Probing anomalous $t\bar{t}Z$ interactions with rare meson decays arXiv:1408.0792.